Design and Development of Solar Based Fast Charger for E-Vehicle Using MPPT Algorithm

Aayush Patidar*, Vijay Kumar Dubey**‡, Dipali Sarvate***

*Department of Electrical Engineering, Prestige Institute of Engineering Management and research, Indore, India

** Department of Electrical Engineering, Prestige Institute of Engineering Management and research, Indore, India

*** Department of Electrical Engineering, Prestige Institute of Engineering Management and research, Indore, India

(ayupatidar@gmail.com, vijaydubeyy@gmail.com, dsarvate@piemr.edu.in)

‡Corresponding Author; Aayush Patidar, Prestige Institute of Engineering Management and research, Indore, India,
Tel: +91 7509781787, ayupatidar@gmail.com

Received: 17.07.2023 Accepted:12.08.2023

Abstract- This paper relates with the Solar based fast charger for e-Vehicle. Currently, Solar Energy based e-vehicle charging make drastic change in dependence on fossil fuel. Charging of e-vehicle are ideally assumed within 2-4 minutes like gas station but in reality, it took more than a hour to fully charge a battery. The paper give an design solution for MPPT based fast charger, focus mainly on the charging rate, energy efficiency and the reduction in power consumption compare to the traditional street e- vehicle charging system. This paper part covered in MPPT Algorithms and Atmega328P microcontroller having the function of Complementary Wave Generator which has been utilized for producing the High resolution PWM signal that further operating the Synchronous Buck Converter. The converter circuit contain an extensive novel interlocking method for protection against Overvoltage, Under Voltage Protection, and Reverse Current & Opposite Polarity. Energy efficiency plays a crucial role in this paper, with particular emphasis on the dusk to dawn voltage as a significant parameter. To address this, several modifications have been made from a hardware design perspective. However, incorporating these protective measures poses challenges when implementing the maximum power point tracking algorithm to extract the maximum power from the solar panel. The MATLAB 2016A software has been utilized to develop the proposed model, and the simulation results and related circumstances are detailed in the result and discussion section.

Keywords DC-DC converter; Maximum Power Point Tracking; Photovoltaic System; Advance converter topology; Start up and Running interlocks.

1. Introduction

All nations share a fundamental requirement to access Sustainable and Cost-effective energy, which is crucial for their economic and Manufacturing expansion, as well as societal and human growth. India holds the third position globally as both a major producer and consumer of energy. According to records from the National Electric Grid, India had already installed and operationalized approximately 370 GW of capacity by March 31, 2020. In the fiscal year 2018-19, India generated an estimated 1372 TWh of electrical energy for utility areas and 1547 TWh when non-utilities were included. The per capita gross electrical energy generation in 2018-19 stood at 1191 kWh.

India has various sources of electrical supply, as depicted in Fig.1, presenting ample opportunities in non-conventional energy sources. However, an essential aspect is efficient power conversion from the energy source to storage devices or loads [1]. Stand-alone applications have emerged as highly profitable systems from an energy supply perspective. Several PV module integrated converters have been developed for high efficiency in stand-alone systems [3]. Micro-grid applications are also successfully meeting energy requirements in various villages across India. Notably, when implementing the CCM (Continuous Conduction Mode) operation in a converter that transfers energy from source to load, stand-alone applications play a critical role in determining the switching frequency boundary condition [3][5].

To fulfill this purpose, various methods are employed for solar energy harvesting. For instance, the Fractional Open Circuit Voltage method [2] considers the ratio of the

maximum peak voltage to the open-circuited voltage to control the system. Additionally, other algorithms have been developed and practiced in recent years, such as the Perturb and Observe (P&O) method [4][5]. Although this method operates efficiently, it exhibits significant output oscillations at the maximum power point (MPP). To address this issue, the Incremental Conductance algorithm [5][10] has been employed, which utilizes variations in the conductance of the PV cell. The Prediction Model-Guided Jaya Algorithm [11], utilized extensively over the past 5 to 6 years, assists in determining the exact MPP. The Fuzzy Logic algorithm [8] is also a popular method, particularly when working with a digital controller, as it effectively regulates the converter under partially loaded conditions [9].

The market offers a range of lithium-ion cell variants, including small cylindrical cells (with a solid body and no terminals), large cylindrical cells (with a solid body and terminals), flat or pouch cells (featuring a soft, flat body), and rigid plastic case cells with large threaded terminals. The latter two variants are sometimes referred to as prismatic cells due to their rectangular shape. These batteries exhibit specific energy densities ranging from 100 to 250 Wh/kg, volumetric energy densities ranging from 250 to 680 Wh/L, and specific power densities ranging from 300 to 1500 W/kg. Lithium-ion cells incorporating a positive electrode of lithium iron phosphate and a negative electrode of graphite typically exhibit a nominal open circuit voltage of 3.7 volts and a typical charging voltage of 3.6 volts. They possess a volumetric energy density of 220 Wh/L (790 kJ/L) and a gravimetric energy density of over 90 Wh/kg. These batteries have a cycle life of 2000-7000 cycles to 80% of the original capacity at 100% depth of discharge (DOD), and over 10,000 cycles to 80% of the original capacity at 10% DOD. The cathode composition consists of approximately 90% C LiFePO4 (phos-dev-12 grade), 5% carbon (superior graphite), and 5% poly-vinylidene fluoride. The cell configuration comprises a carbon-coated aluminium current.

2. System Design

The system comprises a 1000W Solar Panel, a LiFePO4 battery with a nominal voltage of 12.8V, and a load consisting of a e-vehicle charger. The simplified hardware architecture is illustrated in Fig.1.

2.1 Solar Panel:

For experimental purposes, a 60W Mono-crystalline Solar Panel from CENTYSIS is incorporated into the system. The solar panel specifications include an Open Circuit Voltage of 22.2V, a Short Circuit Current of 3.56A, an efficiency of 14.22%, a current temperature coefficient of 0.06, and a voltage temperature coefficient of -0.34. Fig.4 displays the I-V (current-voltage) and P-V (power-voltage) characteristics of the solar panel. At an irradiance level of 1000 W/m2, the PV cell can generate an output of over 1000W.

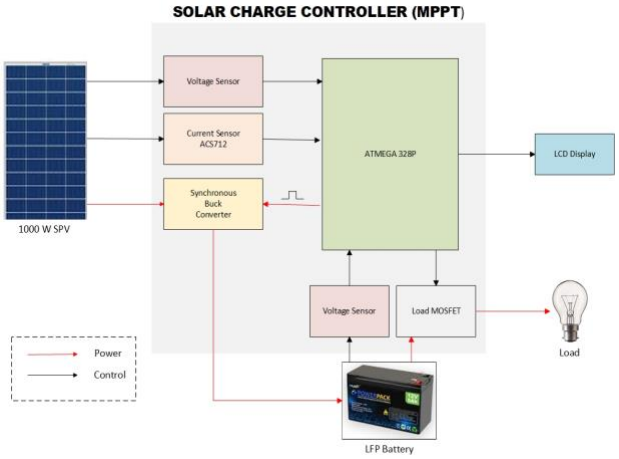

Fig. 1. Simplified Architecture of Hardware

The figure also presents the general model of a solar cell, which is based on a single diode model. The expression for this single diode model is as

$$I = I_{PH} - I_{REV}\left[e^{\frac{V_D + IR_{SS}}{\propto V_T}} - 1\right] - \left(\frac{V_D + IR_{SS}}{R_{SP}}\right) \qquad (1)$$

R_{SP} – The Resistance in Parallel

R_{SS} – The Resistance in Series

I_{PV} –Photocurrent

V_D – The Diode Voltage

a – Ideality Factor

V_T – Thermal Voltage

But if many cells are taken in series and parallel, then the equivalent expression for determining the photocurrent is as follow

$$I = I_{PH}N_P - I_O N_P\left[e^{\frac{\left(V + IR_S\left(\frac{N_S}{N_P}\right)\right)}{a\,V_T N_S}} - 1\right] - \left[\frac{V + IR_S\left(\frac{N_S}{N_P}\right)}{R_P\left(\frac{N_S}{N_P}\right)}\right] \qquad (2)$$

Where N_P is the no. of cells in Parallel & N_S is the no. of cells in Series.

2.2 ATmega328P Microcontroller:

This microcontroller is an 8 – bit, 28 – Pin Flash High Performance RISC CPU based 32KB ISP Flash memory with read-while-write capability. It has C-compiler optimized architecture, 20MHz Internal Oscillator. We get the feature of Software Selectable Frequency range from 20MHz to 31 KHz, 10 – Bit 6 channel ADC pins,1K bytes EEPROM, 2 K bytes SRAM,4 PWM Generating PINs, 1 Complementary Wave Generator Pin, & with ab programmable watchdog timer with internal oscillator. Most of the PIN configured in this project, its Wide Operation Voltage Variant 'F' recommended from 2.3 V to 5.5 V whereas extreme Low Power (XLP) 'LF' Variant is 1.8V – 5.5V. Basically we have objective to implement whole operation in single system. The controller has to work for measuring the voltage and current which will provide input to MPPT algorithm [17] and

then it has to operate in function of Bulk Charge Mode,

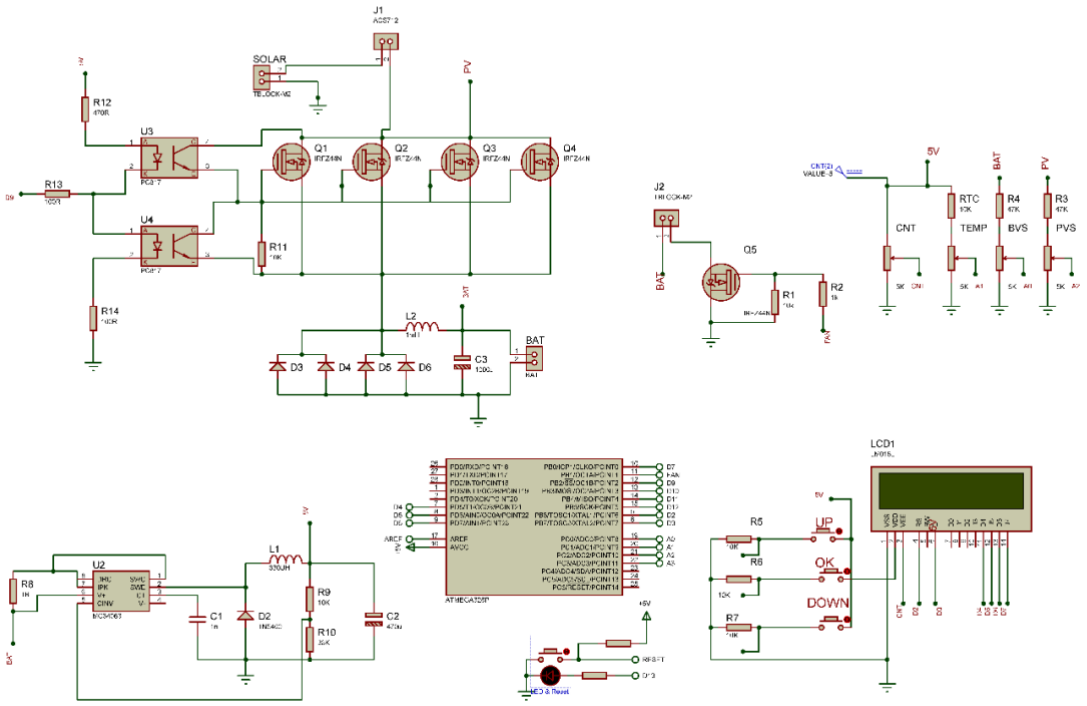

Absorption Mode & then

Fig. 2. Buck Converter from PV cell to 12.8 LPF Battery

float mode. To ensure the long-term reliability of the system, in addition to leveraging the operational features mentioned, a safety circuit is implemented. This circuit is responsible for maintaining the system's reliability. All input/output (IO) ports of the system have a source/sink rating of 25 mA. There are three timers in the system: TMR0 and TMR2 are 8-bit timers, while TMR1 is a 16-bit timer. This microcontroller is having special feature which we discussed earlier that is Internal Oscillator that is the reason we don't need to configure the microcontroller through external oscillator circuit. This increases the overall reliability of the system.

2.3 LM2950 Voltage Regulator IC:

The LM2950 provided constant voltage to Microcontroller and other part of control circuit initially during start up of System. This IC provides 1V to 5V power signal to controller.

2.4 Battery Charging Circuit:

There are two Power MOSFET IRFZ44N M1 & M2 are being used to develop the feature of BUCK Converter from Solar Panel to Battery as shown in Fig.3. The MOSFET Gate to Source Voltage is 20 V, the drain current Id is 49A and RDSON is 17.5 m-Ohm [16]. Based on these basic features further driver circuit designed. [1][2]. the battery voltage is based on the duty cycle D as given in below expression.

$$D = \frac{dV_{BAT}/dt}{dV_{VP}/dt} \tag{3}$$

The resistance R44 and R43 are feeding the required power signal to the M1 and M2 MOSFET due to which the circuit get into the operation mode and battery start charging but MOSFET U32 makes VGS= 0 due to which circuit isolate for some time. This feature of circuit used with MPPT algorithm to achieve the goal. The MOSFET U28 is the device which is getting the PWM signal from the microcontroller while there's another diode D31 is 1N4007 ZENER diode which is working in the system to provide the over-charge protection.

2.5 Driver Circuit:

The other two Power MOSFET M7 & M14 from Battery to e-vehicle charging are being used for developing the feature of BUCK topology as shown in Fig..2. The e-vehicle charging requires always constant current operation because small change in voltage leads to drastic change in current. U27, U26 & U25 are part of driver circuit which is driven by PWM signal generated by Microcontroller. we get high power e-vehicle charging range varying from 10 W to 100 W. For 10 W of e-vehicle charging requires typical drive of 3.4V at 350 mA to generate full charging. The maximum current is 500 mA for the driver circuit. This is the limit for the circuit; even if it is increasing for short pulse duration

may result in damage of circuit. For 30 W module, similar circuit can be used but specification will be different i.e. 700 ma for full brightness output and 1A for maximum current drive for the circuit. [3]

3. Control Algorithm Implementation

The control algorithm utilized in this system primarily consists of a Maximum Power Point Tracking (MPPT) algorithm. However, the circuit features can be divided into two parts:

- Battery Charging Algorithm
- Artificial Neural Network Algorithm

Artificial Neural Network Algorithm (ANN): The controller incorporates a P&O algorithm in each mode, aiming to maximize power generation for battery charging [4]. Different set points are implemented in the controller, enabling all three modes depicted in Figure 6, and facilitating the operation of the Perturb and Observe Algorithm. The duty cycle is adjusted in each mode to execute the algorithm. The flowchart for the Perturb and Observe Algorithm is illustrated in Fig.3. The duty cycle is varied to increase or decrease the output voltage of the converter. During each iteration, the algorithm examines the current power state (P(t)) and voltage state (V(t)), as well as the previous power state (P(t-1)) and voltage state (V(t-1)). Based on these values, the algorithm determines the necessary adjustment to the reference duty cycle in order to track the Maximum Power Point.

3.1 Battery Charging Algorithm:

It is divided into three modes, as depicted in Figure 3:

1. *Bulk Charging Mode:* In this mode, the controller senses the battery voltage, which typically falls between 10.8V and 12.8V. The controller charges the battery up to 80% of the short-circuit (SC) current.
2. *Absorption Mode:* When the battery is already charged above its nominal voltage of 12.8V, the charge controller switches to the constant current charging mode. The voltage level is maintained until the battery is fully charged. At this level, the battery can be used to power loads, but during daytime when lighting loads are unnecessary, the LiFePO4 battery can be charged up to its over-voltage level of 14.2V.
3. *Float Charging Mode:* The third mode of the algorithm is the float charging mode. In this mode, the battery charge is maintained between 13.5V and 14.2V. This condition is considered a floating point condition, where the battery consumes a very low amperage.

These three modes of operation allow for efficient charging and maintenance of the LiFePO4 battery, ensuring optimal utilization and longevity.

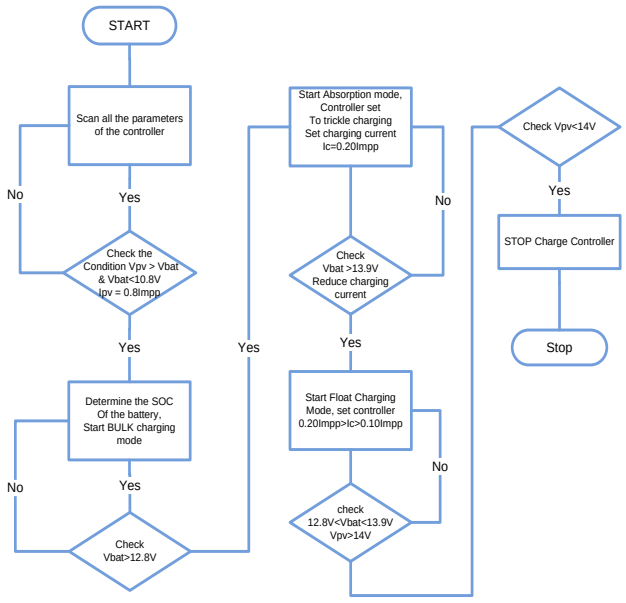

Fig. 3. Battery charging Algorithm

4. Result and Discussion

Figure.3 presents the final result output of the battery charging and discharging profile. The graph illustrates the State of Charge (SOC), which increases from 78.42% to 78.47% during the battery charging process. Simultaneously, the battery current increases from 0 Amps to 3.2 Amps. The negative values shown in the battery charging graph indicate that the battery is in a charging state. When the battery supplies current to the load, the current value becomes positive.

The charging voltage also increases from 13.3V to 13.5V. Since the battery is fully charged, the controller operates in the Float charging state, maintaining a constant voltage level.

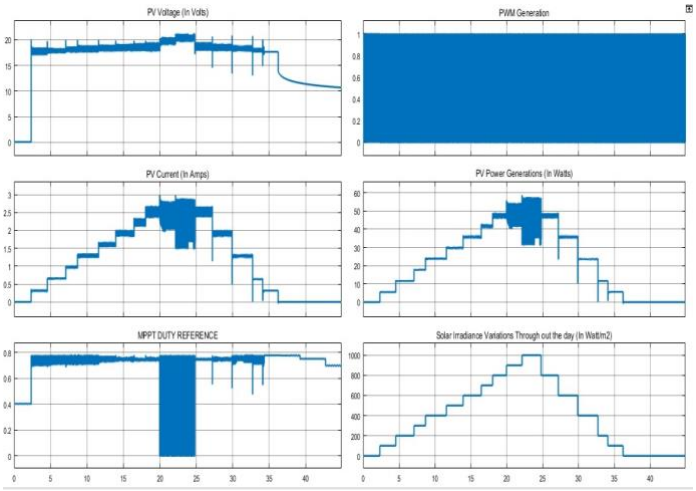

Fig. 4. Simulation Result of the MPPT tracking

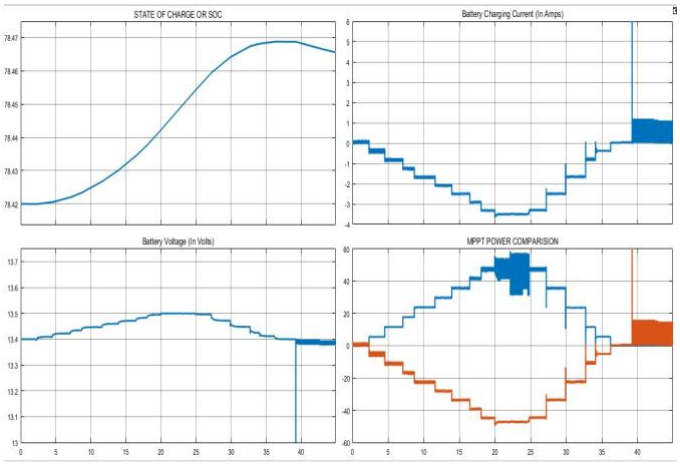

Fig. 5. Simulation Result of the system performance with various features

If we examine the MPPT power conversion, we can observe that the maximum power delivered by the solar panel (represented by the blue line) fluctuates between 55W and 58W. However, the maximum power consumed by the battery ranges from 45W to 50W. This difference is due to the fact that when the battery is in a fully charged condition, it requires minimal charging, resulting in lower power consumption.

Overall, the graph provides insights into the battery charging process, including SOC, current, voltage, and power consumption, highlighting the efficient operation of the system.

When examining the battery discharging characteristic, we plotted the data for various load conditions. The battery was observed to deliver currents ranging from 0.5A to 20A, but our primary interest lies in the discharge characteristic at 0.75A. The physical controller is designed to allow a maximum of 1A during normal night hours and 0.5A during the dimming mode after 6 hours of initial night hours.

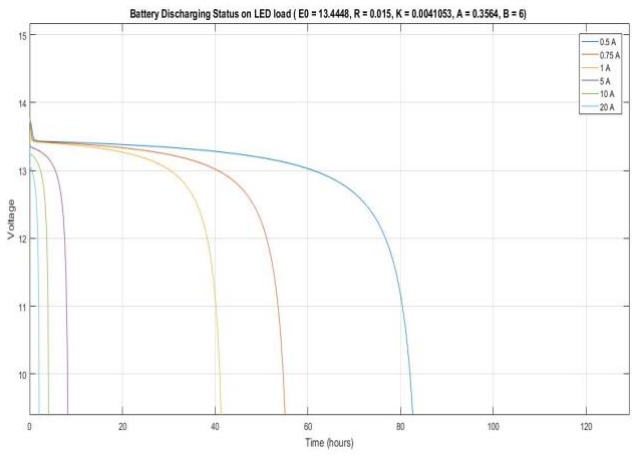

Fig. 6. Battery Discharge Characteristic as per simulation result

Therefore, the average current during the 12-hour nighttime period is 0.75A.

Under this load condition, the battery discharges from 13.7V to 12V over a period of approximately 35 to 40 hours. Since the battery's nominal voltage is 12.8V, this performance aligns with the controller's requirements. It is important to note that the battery's deep discharge voltage is set at 10.8V, and the system is designed for a 3-day autonomy, ensuring that it never reaches the deep discharge condition during the initial stages.

In Fig.6 of the simulation, the battery is observed to discharge from 13.7V to 13.35V between 23 seconds and 36 seconds. This discharge duration is equivalent to approximately 12 hours of discharge condition in the physical battery. This information provides insights into the discharge behavior of the battery, ensuring it operates within the desired voltage range throughout the nighttime period.

Table 1. Experimental Data Recorded

SOC (in %)	Charging Voltage (in Volts)	Discharge Voltage (in Volts)
0		
5		
10	12.8	
15	12.95	12.85
20	13.04	12.9
25	13.13	12.98
30	13.2	13.02
35	13.23	13.07
40	13.25	13.15
45	13.25	13.17
50	13.26	13.18
55	13.26	13.19
60	13.27	13.195
65	13.275	13.2
70	13.3	13.22
75	13.35	13.27
80	13.38	13.3
85	13.4	13.34
90	13.41	13.35
95	13.43	
100	13.48	

In Table 1, the actual data recorded from hardware design, showing only nominal change in discharge and charge cycle of the battery. The same effect has mentioned in Fig.7, where it clearly showing that the charging and discharging cycle are not in similar manner.

Figure 7. Battery charging and discharging curve with respect to the SOC

5. Conclusion

The system becomes very much efficient if we realize all the performance parameter in virtual simulation. Sim-electronics in MATLAB is very much advance library where we can work on real time system. As I did the simulation in MATLAB, I got the same result in hardware, due to which I got the same efficiency in P&O algorithm as you can get in INC algorithm. Therefore this topology for the buck converter has played the significant role to enhance the efficiency of the system. The SOC estimation of Lithium Ion batteries is very difficult. The typical discharge curve of the Lithium Ferrous Phosphate battery, Lithium Manganese Oxide Battery and Lead Acid battery on same voltage level with respect to the DOD of the battery have been mentioned in figure The diagram shows that voltage measurement from 40% to 80% is 6% while in case of LFP batteries, it is only 0.5 V variations. The similar variations have been found in our observation. Lithium Ferrous Phosphate batteries has the advantage of very high level of safety compare to other battery technologies. Due to its High Power density, it is used in various applications like as medium power traction for example robotics, AGV, E-mobility. This is only due to its characteristics. As increasing demand of Stand-Alone Solar system to meet the power requirement has led to the revolution in non-conventional energy source technology.

As it improved the charging experience for EV users, may increase convenience and reduced charging time can incentivize more individuals to switch to electric vehicles.

The implementation of fast chargers utilizing MPPT algorithms has the potential to reshape the Indian energy sector's landscape. This transition would necessitate strategic planning, investments in infrastructure, grid modernization, and policy adaptations to ensure a seamless integration of EVs into the transportation network. The changes brought about by this technology could play a crucial role in promoting a progressive environment for EV manufacturing policies by accelerating EV adoption, spurring innovation, and driving sustainable energy practices.

References

1. R. M. Elavarasan, G.M. Shafiullah, S.K. Padmanaban, Nallapaneni M.K., A. Annam, A.M. Vetrichelvan, L M Popa, J.B. Holm-Nelson, “A Comprehensive Review on Renewable Energy Development, Challenges, and Policies of Leading Indian States With an International Perspective”, IEEE Access, Vol. 8, pp. 74432-74457, Apr. 2020.
2. M. Adley, Kai Strunz, “Irradiance-Adaptive PV Module Integrated Converter for High Efficiency and Power Quality in Standalone and DC Microgrid Applications”, IEEE Transaction on Industrial Electronics,vol. 65, no. 1, pp. 436-446, Jan-2018.
3. V. K. Dubey and S. K. Sharma, "Efficient Driver Circuit Design ameliorating MPPT Tracking at Solar based Lithium Ion Battery Charging," 2022 IEEE Delhi Section Conference (DELCON), New Delhi, India, 2022, pp. 1-8, doi: 10.1109/DELCON54057.2022.9753385.
4. K. Nunotani, F. Yoshida, Y. Kamiya, Y. Daisho, K. Abe, M. Kono, H. Matsuo, “Development and Performance evaluation of Lithium ion Phosphate Battery with superior rapid changing performance”, 2011 IEEE Vehicle Power and Propulsion Conference, Chicago, USA, Sept 2011.
5. J.T.D.C. Neto, A.O. Salazar, A. S. Lock, “Design and Operation of an OCC-based scheme for Stand-Alone PV system powering the DC Load”, IET Renewable Power Generation, Vol 13, no. 12, Sept 2019.
6. J.J. Soon, K. Low, “Optimizing Photovoltaic Model for Different Cell Technologies Using A Generalized Multi-dimension Diode Model”, IEEE Transactions on Industrial Electronics, Vol. 62, no. 10, pp. 6371-6380, Oct. 2015.
7. K.J. Sauer, T. Roessler, C.W. Hansen, “Modeling the Irradiance and Temperature Dependence of Photovoltaic Modules in PVsyst”, IEEE Journal of Photovoltaics, pp. 152-158, Nov. 2014.
8. F. Reis, C. Guerreiro, F. Batista, T. Pimental, M. Pravettoni, J. Wemnes, G. Sorasio, M.C. Brito, “Modeling the Effects of Inhomogeneous Irradiation and Temperature Profile on CPV Solar Cell Behavior”, IEEE Journal of Photovoltaics, Vol. 5, no. 1, pp. 112-122, Jan. 2015.
9. E.I. Batzelis, S.A. Papathanassiou, “A Method for the Analytical Extraction of the Single-Diode PV Model Parameters”, IEEE Transactions on Sustainable Energy, Vol.7, no.2, pp. 504-512, Dec. 2015.
10. I.A. Ibrahim, Benjamin C. Duck, Christopher J. Fell, “An Adaptive Wind Driven Optimization Algorithm for Extracting the Parameters of Single Diode PV cell

model", IEEE Transaction on Sustainable Energy, vol. 11, no 2, pp 1054-1066, Apr 2020.

11. G. R. C. mouli, J. Schijffellen, M.V.D.Heuvel, M. Kardolus, P. Bauer, "A 10kW Solar-Powered Bidirectional EV Charger Compatible with Chademo and COMBO", IEEE Transactions on Power Electronics, vol. 34, no. 2, pp. 1082-1098, Feb. 2019.
12. Andrea Montecucco, Andrew R. Knox, "Maximum Power Point Tracking Converter Based on the Open-Circuit Voltage Method for Thermoelectric Generators", IEEE Transaction on Power Electronics, vol 30, no 2, pp 828-838, Feb 2015.
13. N. MOHAN, T. UNDELAND, and W. ROBBINS, Power Electronics: Converters, Applications, and Design, 2nd edit., New York: John Wiley & Sons, 1995, Chapters 19-26.
14. R. W. Erickson, Dragan Maksimovic, Fundamentals of Power Electronics, 2nd Edit., Bouldor, Colarado: New Yiork: Cluver Academic Publisher, 2001, Chapter 1-10.
15. S. Teleke, M.E.Baran, S. Bhattacharya, A.Q. Huang, "Rule-Based Control of Battery Energy Storage for Dispatching Intermittent Renewable Sources", IEEE Transactions on Sustainable Energy, vol.1, no.3, pp.117-124, Oct. 2010.
16. Al Khas, A. and Cicek, I., 2019, November. SHA-512 based wireless authentication scheme for smart battery management systems. In 2019 8th International Conference on Renewable Energy Research and Applications (ICRERA) (pp. 968-972). IEEE.
17. Harighi, T., Bayindir, R. and Hossain, E., 2018. Overviewing quality of electric vehicle charging stations' service evaluation. International Journal of Smart Grid-ijSmartGrid, 2(1), pp.40-48.